IEEE Access
Multidisciplinary | Rapid Review | Open Access Journal

Received August 31, 2018, accepted September 18, 2018, date of publication September 24, 2018, date of current version October 19, 2018.

Digital Object Identifier 10.1109/ACCESS.2018.2871818

A Compact Printed Monopole Antenna With Wideband Circular Polarization

MD. SAMSUZZAMAN[1,2], (Member, IEEE), MOHAMMAD TARIQUL ISLAM[1,3], (Senior Member, IEEE), AND MANDEEP JIT SINGH[1], (Member, IEEE)

[1]Center of Advanced Electronic and Communication Engineering, Universiti Kebangsaan Malaysia, Bangi 43600, Malaysia
[2]Department of Computer and Communication Engineering, Patuakhali Science and Technology University, Patuakhali 8602, Bangladesh
[3]Laboratory of Spacecraft Environment Interaction Engineering, Kyushu Institute of Technology, Kitakyushu 804-8550, Japan

Corresponding authors: Md. Samsuzzaman (samsuzzaman@siswa.ukm.edu.my) and Mohammad Tariqul Islam (tariqul@ukm.edu.my)

This work was supported by the University Research Grant under Project MI-2017-001.

ABSTRACT In this paper, a novel compact circularly polarized (CP) monopole wideband printed patch antenna is proposed. The antenna consists of a hook-shaped branch connected at the partial rectangular ground plane and reversed unequal arm with an L-shaped microstrip-feed which helps the antenna achieve wideband circular polarization property. The measured results display that the proposed compact ($44 \times 44 \times 1.6$ mm^3) antenna acquires 3.12 GHz (56%, 2.25–4.0 GHz) at the 10-dB impedance bandwidth, and the axial ratio (AR) bandwidth at 3-dB is 3.48 GHz (63.61%, 2.38–4.60 GHz). A parametric study of different design parameters and measured and simulated results of the various characteristics of the designed antenna is presented to verify the performance of the radiation mechanism. Finally, by scaling only, the dimensions of the proposed antenna without changing another parameter, a wide impedance and AR bandwidth are achieved. On account of the simple planar structure and scaling dimension with broadband CP property, the proposed antenna does apply in a variety of wireless communication systems such as ISM, WiMAX, WLAN, satellite communications, cordless telephones, weather radar systems, and lower frequency bands CP type applications.

INDEX TERMS Axial ratio, compact, circular polarization, hook-shaped, planar printed antenna, wideband.

I. INTRODUCTION

In recent years, the popularity of circularly polarized microstrip antennas have been increasing due to several modern wireless communications, such as satellite communications, WLAN(Wireless Local Area Network) and WiMAX (Worldwide Interoperability for Microwave Access), RFID (Radio-frequency identification) readers and GPS (Global Positioning System), while it is used as both transmitter and receiver due to its flexible orientation [1]. The techniques to enhance the cross polarization of CP antennas at equally the transmitter and receiver ends for increased discrimination enhances the invulnerability to multipath propagation. The demand for CP antennas that have a wide operating bandwidth and wide AR band are increasing with the current high demand for high-speed wireless communication.

Numerous forms of antennas having different patch shapes, feed lines and slots in the ground and a patch that can considerably generate wideband CP characteristics have been described in the literature. Circular polarization can be achieved using the trepidation of a thin slot or a curtailed stub in a microstrip patch [2], [3]. To achieving 19.8% of the impedance bandwidth and 19.3% of the 3 dB AR bandwidth, two monopolar modes of a circular patch are connected with an altered ground plane through a set of conductive vias [4] which increases the complexity of the design. The antenna reported in [5] has an asymmetrical dipole, which is fed by an L-shaped microstrip transmission line and the ground is slotted, which acquired an AR bandwidth of 23%. An annular slot antenna is reported with two connected annular slots that have achieved an AR bandwidth of 46.7% at 3 GHz [6]. An inverted L-shaped slot-loaded ground plane and an inverted U-shaped strip achieved 60% of the wide axial ratio [7]. With dimensions of 72 mm $\times$ 148 mm $\times$ 1.6 mm, a rectangular radiation patch placed asymmetrically to the microstrip line achieved 136% of the impedance bandwidth and 77% of the AR bandwidth [8]. Zhang *et al.* [9] introduced a CPW fed antenna where the AR bandwidth is extended 44.9% from 4.58 GHz to 7.23 GHz, developing one

of the two requisite orthogonal apparatuses together with the monopole for the CP. For exciting a monopole along with a slot in parallel, a branched microstrip structure was used to achieving circular polarization with dimensions of 38 mm × 54 mm. The impedance bandwidth(−10 dB) and AR bandwidth (3dB) of the branch patch antenna were above 73% and 46.8%, respectively [10]. With a profile of 24λ, successively swapped strips that connect with a cross dipole and achieved 23% of the bandwidth (2.3-2.9 GHz) at a 3 dB AR. A 51.4% AR bandwidth from 1.82 to 3.08 GHz is achieved with a modified ground and two orthogonal edges of the rectangle that produce CP, which was fed asymmetrically [11]. The CP bandwidth of approximately 61.96% has been achieved with an inverted asymmetric arm L-shaped microstrip and partial ground plane, but the dimensions of the antenna were $54 \times 54 \times 1.6$ mm^3 [12]. The wideband antenna fed by the M-probe achieves 16.8% of the AR bandwidth [13]. With a height of 0.1λ, the above antenna shows the CP band. However, due to the stacked parasitic patch, the wideband is partial. An enhanced CP band of 16% is adopted with a probe-fed CP patch with a coplanar parasitic ring [14]. A CPW-fed widened patch antenna having a nesting-L slot was previously proposed [15]. By protruding an asymmetric T-type strip from the CPW feed line, a 110% input impedance bandwidth was achieved. A nesting-L slot structure was familiarized to widen the CP radiation bandwidth on the ground with overall dimensions of 80×80 mm^2. Shen et al. introduced an asymmetrical Y-shaped feeding line patch antenna to generate CP radiation for X-band applications, and a through via that is in series with an inductive strip was employed to achieve the impedance bandwidth of 31.4% in which the AR is less than 2 dB [16]. More recently, a wideband circular polarized printed triangular monopole antenna was proposed [17]. An asymmetrical excitation of a trilateral ground plane and a planar triangular monopole wideband produces circular polarization. A wide AR bandwidth covering 62% (1.42 GHz −2.7 GHz) is provided for combined CP radiation. Though the antenna does not cover a compact dimension. The overall dimensions of the antenna are 79.2×112 mm^2. A moon-shaped antenna [18], a slot antenna [19], and a chifre-shaped monopole antenna [20] with 3 dB AR bandwidths of 40%, 49% and 41.6%, respectively, were proposed. A CPW-fed square slot antenna with two asymmetric T-shaped feed lines and an inverted-L grounded strip was stated in [21]. In addition, two Vivaldi antenna elements were cross-placed to shrinkage the antenna dimension and to get broadband CP operation [22], which is a comparatively complex design. Recently, a square slot antenna with an antipodal Y strip [23], a cross-shaped planar antenna with a ground plane extension [24], and compact, wideband directional CP antenna [25] have been offered to achieve a wide impedance and AR bandwidth. However, the majority of the CP antennas mentioned previously possess a 3-dB AR bandwidth of significantly less than 60% with large electrical length. Furthermore, as per the author's knowledge, there have been very few attempts to achieve wideband circular polarization through perturbations of conventional printed monopole/dipoles.

In this article, a new planar simple antenna structure is offered with an inverted L-shaped feed and hook-shaped ground to generate CP. By modifying the fissure between the inverted L- strip and the hook-shaped ground plane and between the length and width of the hook-shaped branch with the partial rectangular ground plane, broadband CP operation is achieved. The high-frequency structure simulator (HFSS) was used to design and optimize the proposed planar monopole antenna. To determine the accuracy of the proposed

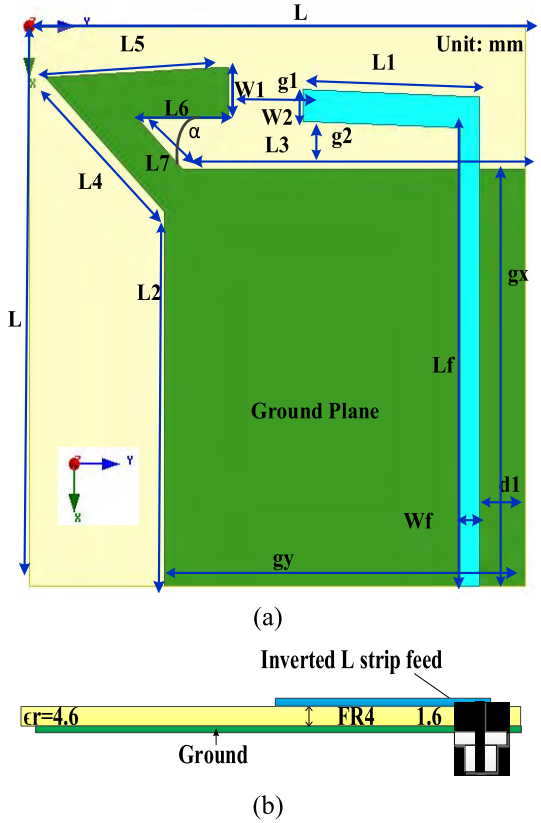

FIGURE 1. Schematic layout of the proposed printed CP antenna: (a) overall design and (b) cross-sectional view.

TABLE 1. Optimized design parameters of the proposed antenna.

Parameter	mm	Parameter	mm	Parameter	mm
L	44	$L3$	37.37	$W1$	3
L_f	36.05	$L4$	20.19	$W2$	6
W_f	2.2	$L5$	21.02	$d1$	5.5
L_1	19	$L6$	9.55	gx	32.8
L_2	35.94	$L7$	7.52	gy	32
$g1$	8.56	$g2$	3.74	α	45°

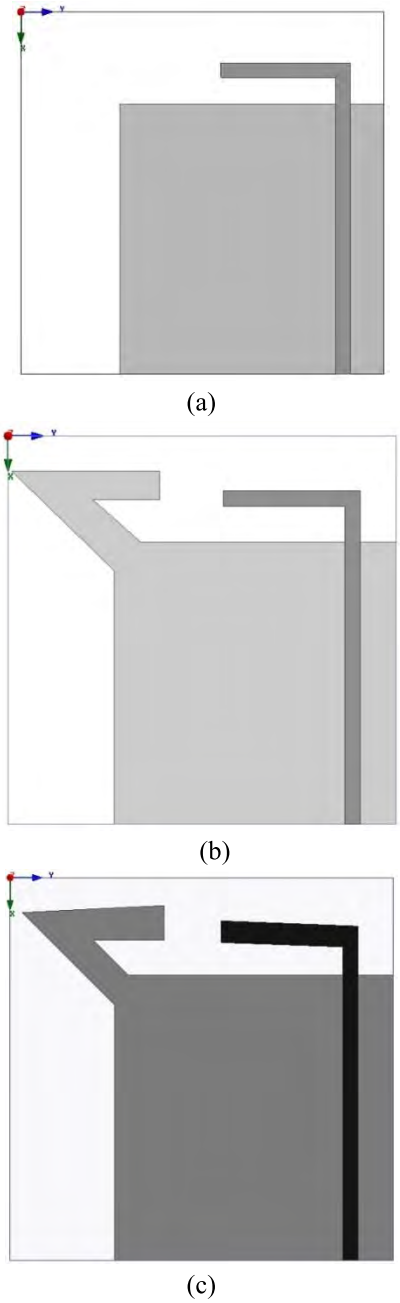

FIGURE 2. Development of the realized antenna for (a) Antenna 1, (b) Antenna 2, and (c) Antenna 3.

antenna, the simulated results are compared with the experimental results. Finally, by scaling only the dimensions (L) of the proposed antenna, a wide impedance (−10dB) and AR (3dB) bandwidth are achieved. So, any researcher can redesign the required CP operating band application antenna with only scaling the dimension (L) of the proposed antenna without altering the other parameters.

II. ANTENNA GEOMETRIC LAYOUT DESIGN

The schematic layout of the proposed antenna is presented in Figure 1. The proposed antenna is fabricated on a low-cost

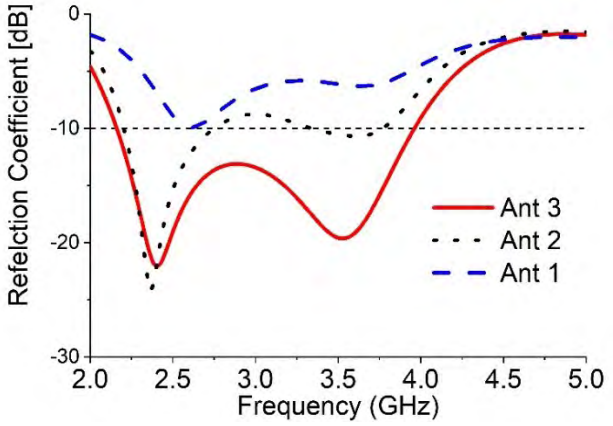

FIGURE 3. Numerical S_{11} for Antenna 1, Antenna 2 and Antenna 3.

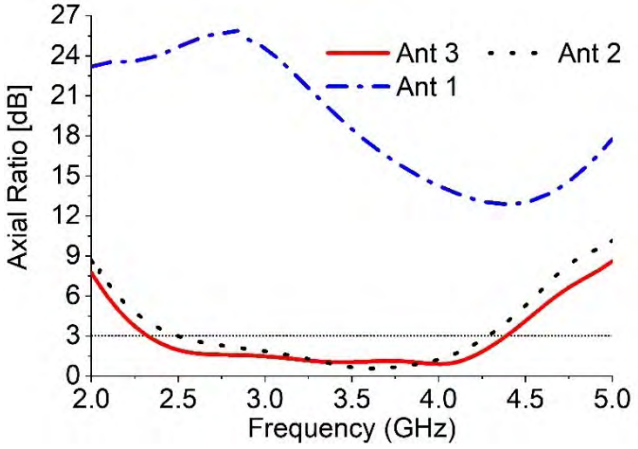

FIGURE 4. Numerical AR for Antenna 1, Antenna 2 and Antenna 3.

FR4 (epoxy resin glass fiber) substrate material with a height of 1.6 mm and a dielectric constant of $\varepsilon r = 4.6$. The antenna is fed with a 50 Ω SMA (subminiature version A) connector for signal transmit or receive. The presented antenna comprises an inverted asymmetric L-shaped feed line on top of the substrate. The asymmetric inverted L-strip is a traditional monopole antenna with linear polarization excitation. A hook-shaped branch is connected to the partial rectangular ground plane to generate two orthogonal modes with a 90° phase difference. This capacitive, coupled, hook-shaped arm with a partial rectangular shaped ground plane excites the inverted L strips and strongly influence the amplitudes of the two orthogonal modes. Therefore, it is possible to generate CP radiation by tuning the gap width between the hook-shaped vertical arm and the inverted L strip vertical arm. The gap between the partial rectangular ground plane and the inverted L strip also plays an important role for impedance matching. The optimized design parameters of the mentioned antenna structure are listed in Table 1. To justify the development process, four prototypes are presented, as shown in Figure 2. Antenna 1 only contains an inverted L-strip feed

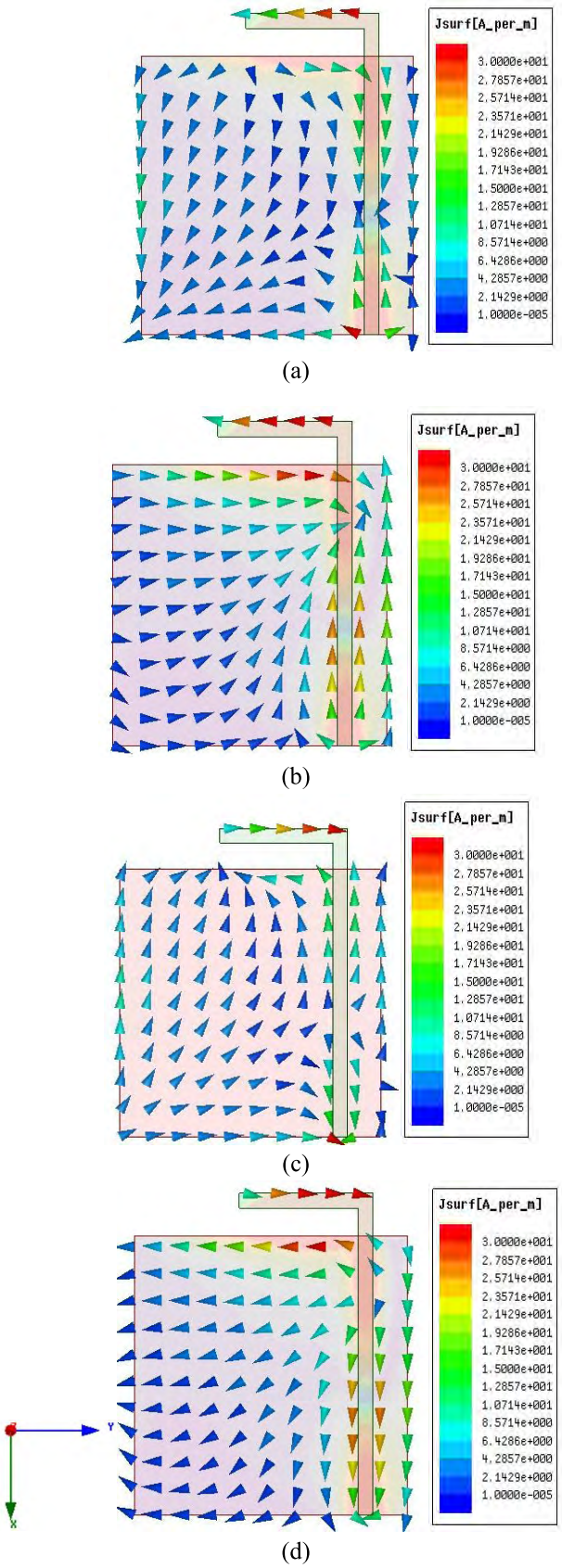

FIGURE 5. Surface current distribution behavior of Antenna 1 (a) 0° (b) 90° (c) 180° and (d) 270° at 3.0 GHz.

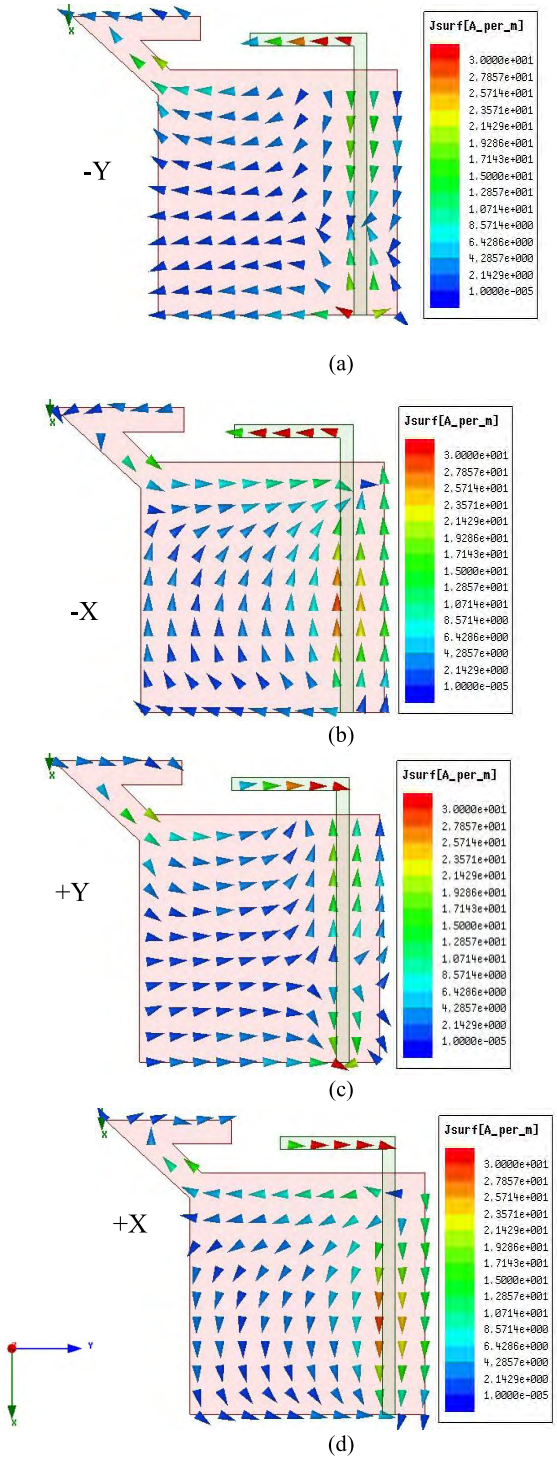

FIGURE 6. Surface current distribution behavior of Antenna 2 (a) 0° (b) 90° (c) 180° and (d) 270° at 3.0 GHz.

line and a partial rectangular ground plane on the bottom layer. Antenna 2 includes an inverted L-strip feed line and a hook-shaped arm connected to the partial rectangular ground plane. Antenna 3 has an asymmetric inverted L strip feeding line and optimized hook-shaped arms connected to the partial rectangular ground plane.

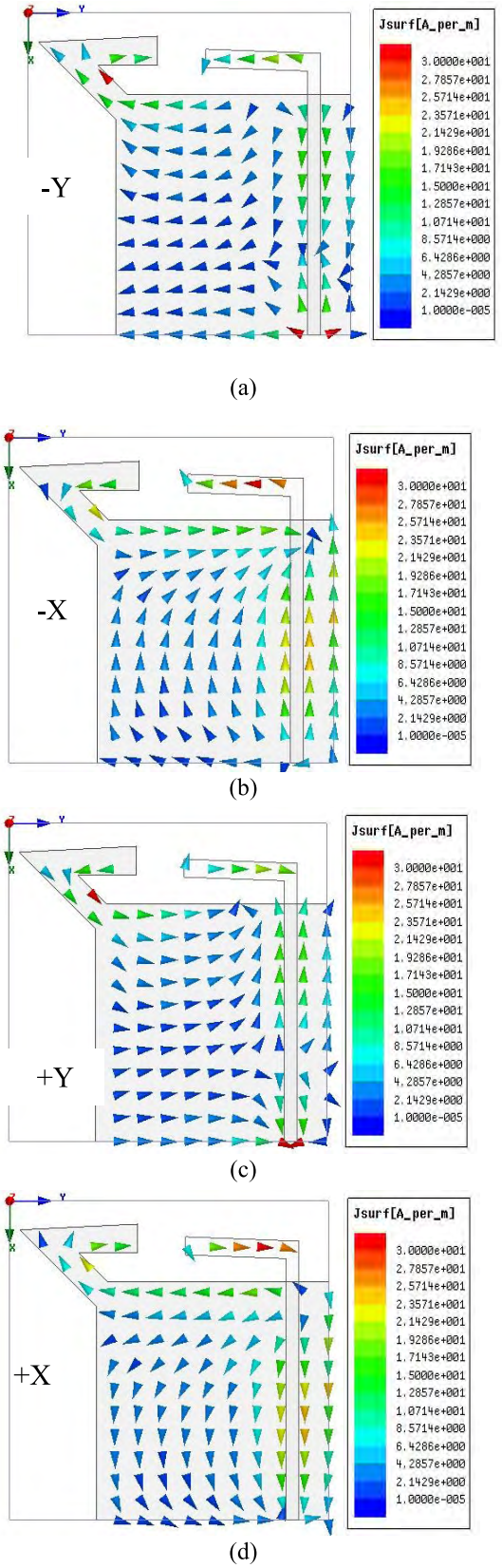

FIGURE 7. Surface current distribution behavior of Antenna 3 (a) 0° (b) 90° (c) 180° and (d) 270° at 3.0 GHz.

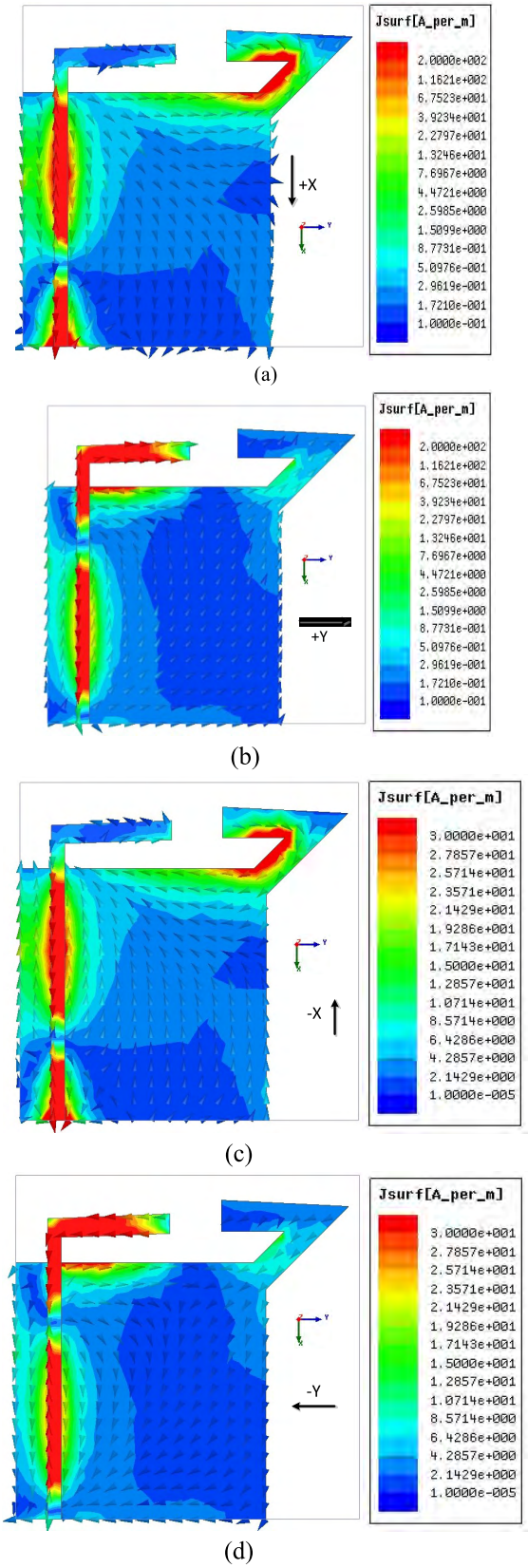

FIGURE 8. Surface current distribution of the mirroring antenna at 3.0 GHz. (a) 0°. (b) 90°. (c) 180°. (d) 270°.

A comparison between Antenna 1 and Antenna 2 can be seen in Figure 3 and Figure 4, where the hook-shaped arms not only improve the 10 dB impedance bandwidth from 0% (Antenna 1) to 21.86% (Antenna 2) at a center frequency

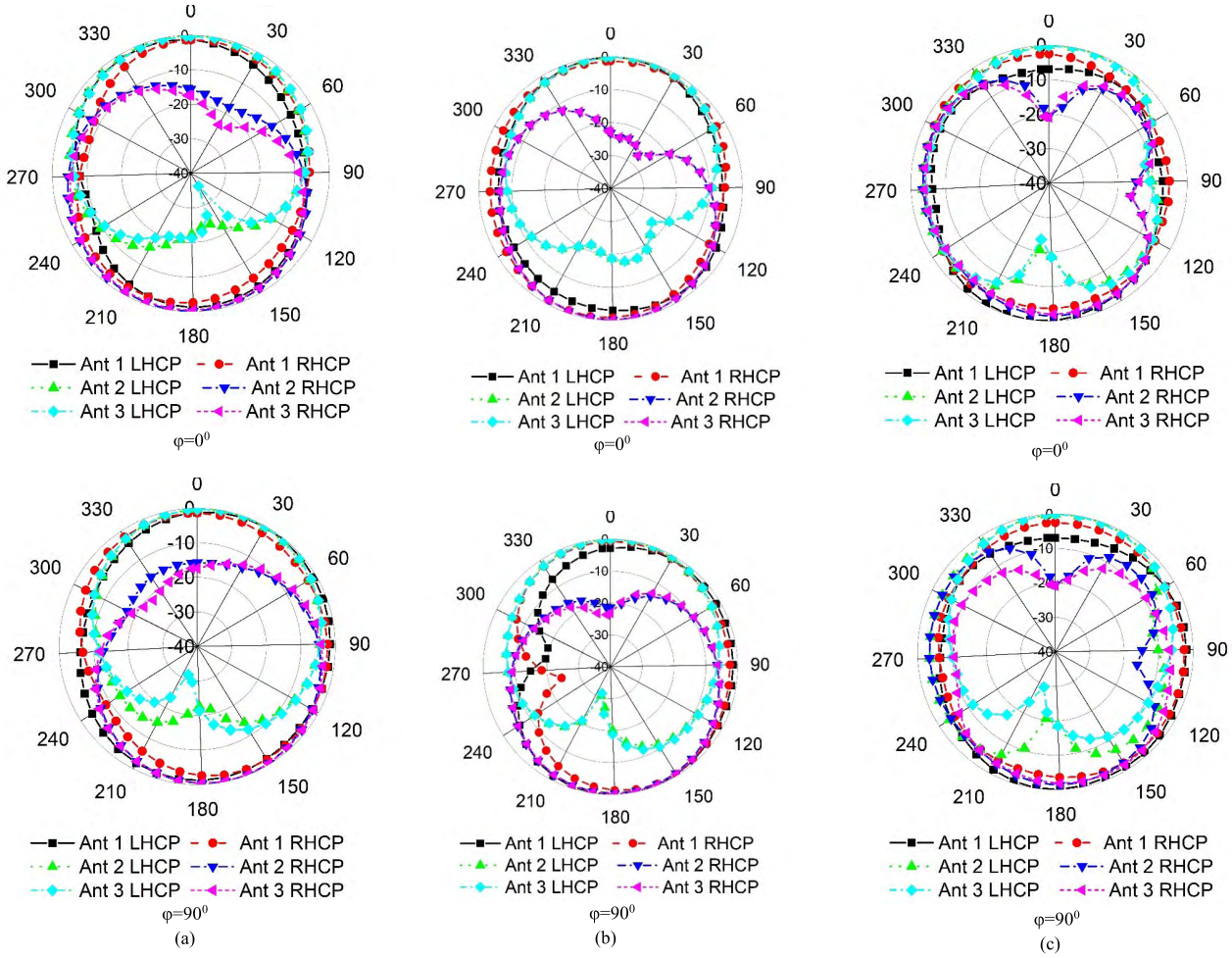

FIGURE 9. Simulated radiation pattern of Antenna 1, Antenna 2 and Antenna 3 at (a) 2.4 GHz (b) 3.0 GHz (c) and 3.9 GHz.

of 2.47 GHz but also create two orthogonal modes with a 90° phase difference. This helps to attain less than a 3 dB axial ratio bandwidth from 0% (Antenna 1) to 52.50% (Antenna 2) with respect to the middle frequency of 3.39 GHz. This phenomenon was investigated using the top and bottom layer current distribution, as depicted in Figures 5, 6, 7 and 8 at 3 GHz for Antenna 1, Antenna 2 and Antenna 3, respectively. It can be seen based on Figure 5 of Antenna 1 that there is no specific variation in the main direction of the current after the phase changes. The inverted L-strip acts as a traditional monopole antenna with stimulation linear polarization. After inserting a hook-shaped branch in the rectangular ground plane, the surface current distribution is altered in Figure 5 for Antenna 2. The main direction of the surface current vector at the rectangular ground with the feed in Figure 6 is towards the −Y direction for the 0° phase, the -X direction for the 90° phase, the +Y direction for the 180° phase and the +X direction for the 270° phase. The hook-shaped branch extends out of the ground but lacks the ground characteristics shown in Figure 6. Instead, it is more similar to a stimulated radiation element. The hook branch disrupts the current distribution of the ground and generates different orthogonal modes every time for CP radiation. The antenna also exhibits broadband performance due to the combination and interaction of the hook-shaped branch and asymmetric inverted L-strip. Finally, the surface current concentration of Antenna 3(proposed) at the four phase angles of 0°, 90°, 180°, 270° at a 3 GHz frequency, shown in Figure 7, can demonstrate the mechanism of the wideband CP radiation. An instant current phase of the antenna at 90° intervals proves the existence of circularly polarized radiation. The current flows rotate right-handed from the −Y-axis to the +X axis and results in left hand circularly polarized (LHCP) radiation along the +Z direction. On the other hand, right-hand circular polarization (RHCP) may be accomplished simply by mirroring the antenna about the XZ-plane. The surface current concentration of mirroring antenna with four phase angles of 0°, 90°, 180°, 270° at 3 GHz frequency, presented in Figure 8, can further demonstrate the mechanism of the wideband CP radiation. An instantaneous current phase on the proposed antenna, at 90° intervals demonstrates a circularly polarized radiation. The current flows rotate anticlockwise from the

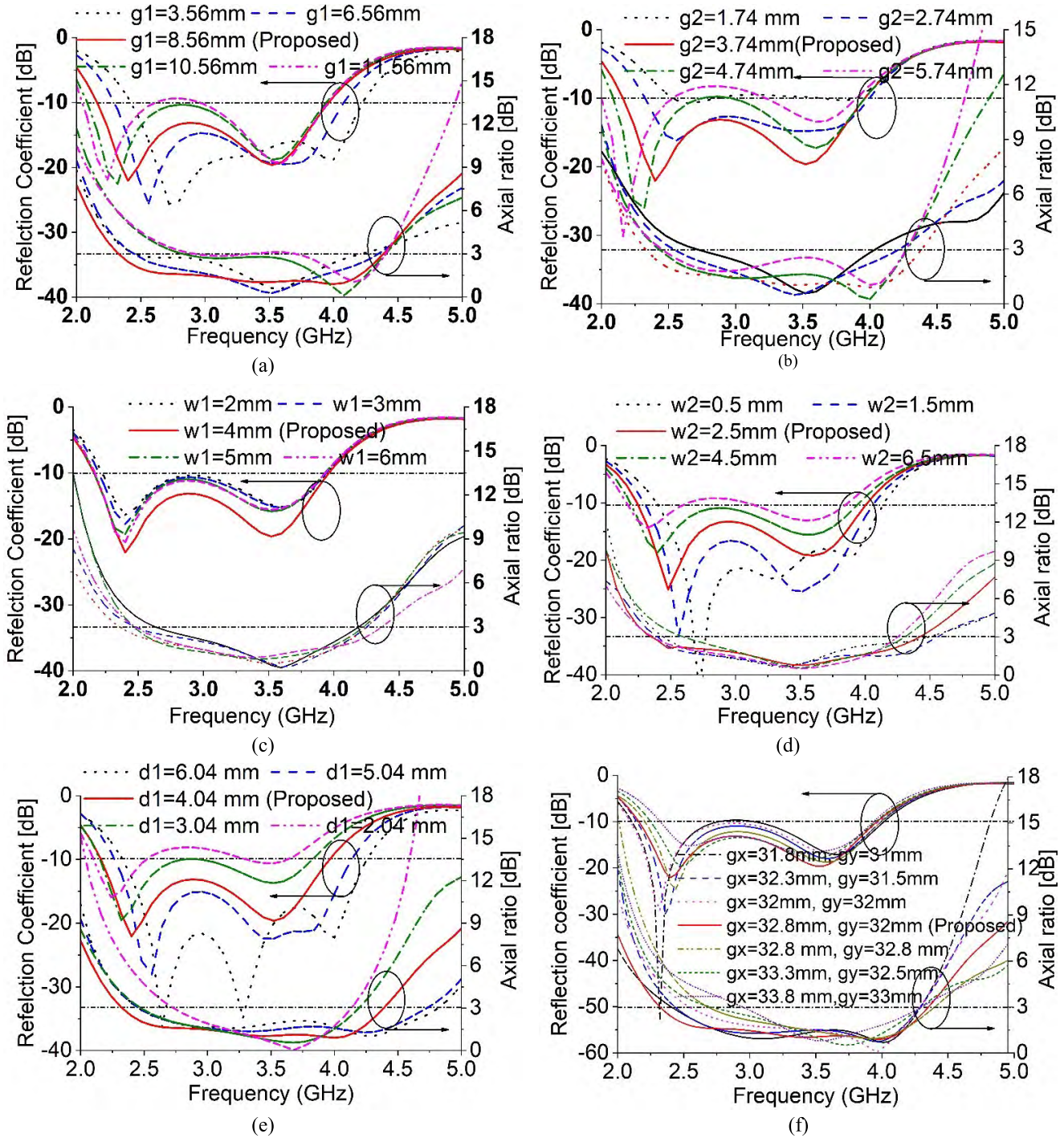

FIGURE 10. Simulated reflection coefficient (S_{11}) and AR with several values of (a) *g1*, (b) *g2*, (c) *W1*, (d) *W2*, (e) *d1* and (*f*) gx, and gy.

+X axis to the −Y axis and result in the RHCP radiation toward the +Z direction.

Comparing Antenna 2 to Antenna 3, it can be perceived in Figures 3 and 4 that by optimizing the dimensions of different parameters, the impedance bandwidth can be extended from 21.86% to 58.40%, and the AR bandwidth can be enhanced from 52.50% to 61.50%. Based on the simulated reflection coefficients of Antenna 1, Antenna 2, and Antenna 3 as depicted in the Smith chart in Figure 3, it can be inferred that the optimized gap and hook-shaped branch length introduce the resonant frequency and impedance bandwidth improvement by merging the different resonant bands. Figure 9 depicts the simulated radiation pattern of Antenna 1, Antenna 2 and Antenna 3 at 3.0 GHz. It can be clearly told

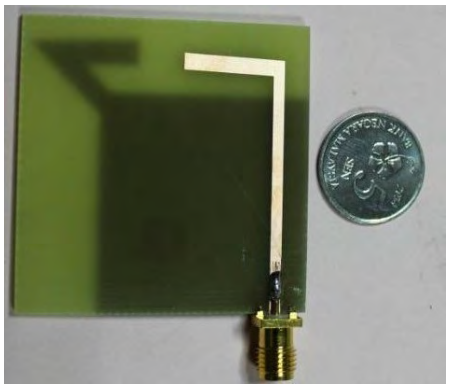

(a)

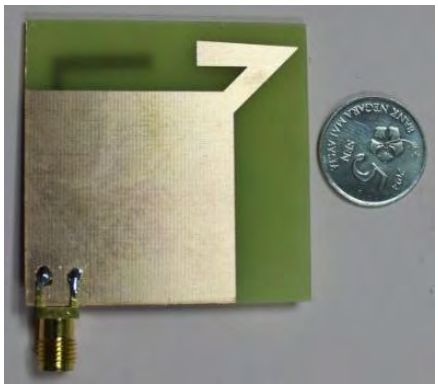

(b)

FIGURE 11. The optimized antenna configuration and its prototype. (a) Top view. (b) Bottom view.

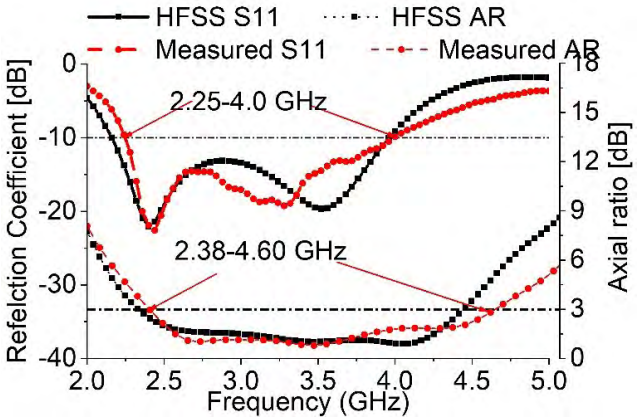

FIGURE 12. Simulated and measured S_{11} and AR vs frequency of the presented CP antenna.

from this figure that Antenna 1 exhibits an omnidirectional radiation pattern whereas Antenna 2 and Antenna 3 exhibit RHCP and LHCP radiation characteristics in both the Phi = 0° and Phi = 90° planes.

III. PARAMETRIC ANALYSIS

To assess the effect of the different antenna parameters on the impedance and AR bandwidth, a parametric study is shown. Figure 10 portrays the simulated S_{11} and AR with different parameter values of g_1, g_2, W_1, W_2, d_1, g_x, and g_y. All the parameters remain fixed at their starting values unless otherwise specified.

A. EFFECT OF GAP LENGTH g1

Figure 10(a) displays the simulated reflection coefficient and AR as functions of different gap lengths denoted by *g1* between the hook-shaped branch W_2 and the inverted L strip width W_1. The greater value g_1 represents the shorter length of both branches. It can be noted from this figure that the resonant frequency or −10 dB impedance frequency shifts to a lower frequency as *g1* increases. On the other hand, the resonant frequency or −10 dB impedance frequency shifts to a higher frequency as g_1 decreases. However, the reflection coefficient in the middle band is extremely deteriorated when g_1 continues to increase. From this figure, it can also be seen that this parameter mainly affects the AR in the lower band. The wide axial ratio with a wide reflection coefficient bandwidth has been achieved using the optimized dimension of $g_1 = 8.56$ mm.

B. EFFECT OF GAP LENGTH g2

Next, the effect of the gap g_2 between the inverted L strip and ground plane arm L_3 is explored, as shown in Figure 10(b). The impedance bandwidth decreases when the gap becomes narrower. This parameter mainly affects the impedance bandwidth of the lower band when the upper band frequency changes slightly. It can be expected that the gap significantly affects the energy coupling between the ground plane and the inverted L-shaped strip. The AR bandwidth shifts slightly to a higher frequency as the gap decreases, because a greater capacitor is obtained.

C. EFFECT OF WIDTHS W_1 AND W_2

From Figures 10(c) and (d), it can be seen that the length of the vertical arm of the hook-shaped branch W_2 and inverted L strip vertical arm length W_1 have a significant influence on the reflection coefficient and slight effects on the AR. By increasing W_1 and W_2, the equivalent of the wide frequency band (2.15 GHz-4.0 GHz) is significantly enhanced. This trend is due to the length of the arms, which can stimulate the coupling of the top and bottom conductors. When the arm lengths are static at $W_1 = 4$ mm and $W_2 = 2.5$ mm, the broadest bandwidth of the presented antenna can be attained.

D. EFFECT OF DISTANCE d1

Figure 10(e) reveals the simulated reflection coefficients and ARs as functions of frequency for different distances of the feed line from the closer vertical edge of the ground plane d_1. With reference to Figure 10(e), the feed distance significantly affects the input impedance. As d_1 decrease from 6.04 to 2.04 mm, the impedance passband shifts downward and AR bandwidth decrease. The optimum distance for the proposed design is given by $d_1 = 4.04$ mm.

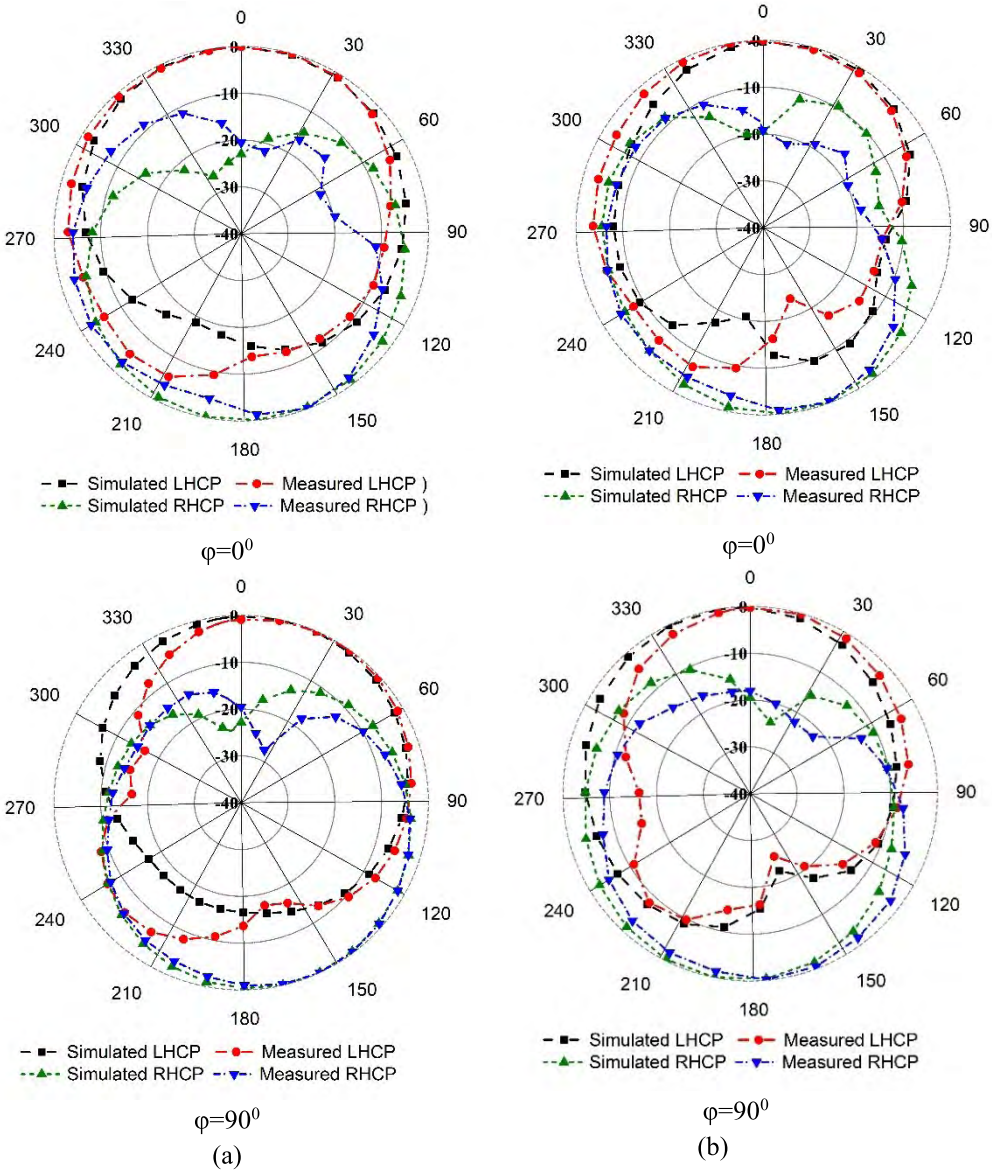

FIGURE 13. Simulated and measured normalized LHCP and RHCP radiation patterns at (a) 2.4 GHz and (b) 3.5 GHz.

E. EFFECT OF THE GROUND PLANE LENGTH g_x AND WIDTH g_y

Finally, the rectangular ground plane length g_x and width g_y exhibit a significant effect on the S_{11} and AR of the antenna, which is portrayed in Figure 10(f). The gap between the ground plane length g_x and the horizontal inverted L stripes introduce a coupling capacitance and play an essential role in boosting the impedance bandwidth. It is seen that by decreasing the values of g_x and g_y, the S_{11} values exhibit better performance at lower frequencies. However, the impedance bandwidth lessens as the g_x and g_y increase. On the other hand, substantial improvement of the AR impedance matching is perceived in the lower frequency band by decreasing the lengths gx and gy of the rectangular ground plane. It is to be distinguished that the ground plane size has little effect on the higher frequency band of the AR bandwidth. For the widest impedance bandwidth and AR bandwidth, values of $g_x = 32.8$ and $g_y = 32$ mm are optimum.

IV. MEASURED RESULT AND DISCUSSION

Optimized proposed antenna prototypes, Antenna 3 is fabricated and measured. The snapshot of the antenna prototype is presented in Figure 11. Investigational results are measured with the Agilent N5227A performance network analyzer and the UKM Satimo Star Lab (Near field antenna measurement system). From the achieved results and depicted in Figure 12, the experimental impedance bandwidth of the reflection coefficient at below −10 dB is approximately 1.75 GHz (2.25-4 GHz), which is approximately 56% regarding the center frequency at 3.12 GHz. The measured 3 dB

TABLE 2. Comparison of the broadband CP antennas.

References	f_c (GHz), f_{cAR} (GHz)	Antenna size in Electrical length at $f_c(\lambda_0^3)$	BW (%)	AR BW (%)	State of the Art (To Achieve Wideband Impedance AR Bandwidth)
[5] 2010	3.3, 3.3 Taconic RF35	0.32×0.39×0.017	41	23	An asymmetrical dipole with a slit in the ground plane which are fed by an L-shaped microstrip feedline using a via.
[6] 2011	3.25,3.00 FR4	0.35×0.65×0.16	61.53	46.7	Two annular ring slots and I strip feed line
[7] 2012	3.02,2.9 FR4	0.48×0.44×0.015	67.76	62.07	Inverted L-shaped monopole, an inverted U-shaped strip, and a slot-loaded ground plane.
[8] 2012	2.65,2.45 RT Duroid	0.63×1.45×0.013	136	77	Rectangular radiation patches placed asymmetrically with respect to the microstrip feed line
[9] 2013	5.66,5.90 FR4	0.49×0.47×.02	76.9	44.9	Rectangle patch, an improved ground-plane and appropriately adding a vertical stub and cutting a horizontal slit on the ground-plane
[10] 2014	3.13,2.78 PTFE	0.35×0.50×1	73	46.8	Triangular monopole and a slot scratched on the ground plane with via
[11] 2014	2.47,2.45 FR4	0.57×0.57×0.026	56.2	51.4	Designing the antenna asymmetrically
[13] 2014	2.54,2.69 FR4	0.494×0.494×0.014	55.40	61.96	Inverted L-strip and slotted ground plane with a shape
[15] 2014	3.19,4.6 FR4	1.227×1.227×0.322	110	60.68	Protruding asymmetric T-type strip from CPW feedline and a nesting-L slot (NLS) structure in the ground
[16] 2014	10.85,10.85 Rogers	0.5×0.5×0.018	31.4	31.4	Asymmetrical Y-shaped feeding line and slotted ground plane with a via
[17] 2015	2.06,1.97 FR4	0.618×0.544×0.010	58	62	Asymmetrical excitation of a triangular ground plane and planar triangular monopole.
[18] 2015	2.91,3.02 FR4	0.705×0.469×0.008	57.28	49	Moon-shaped printed monopole antenna with the modified ground plane
[20] 2016	2.4,2.5 FR4	0.31×0.29×0.008	75	41.6	The chifre-shaped monopole radiator, with asymmetric feed
[19] 2016	6.375 5.75 FR4	0.29×0.29×0.019	90	40	Simply protruding a horizontal stub from the ground plane towards the center of the wide slot, and n feeding the wide slot with a microstrip feedline
[21] 2016	3.38,2.85 FR4	0.40×0.27×0.011	81	59..7	Square slot, two asymmetric T-shaped feed lines in orthogonal direction jut from signal lines, and an inverted-L grounded strip with three straight strips
[23] 2017	3.25,4.4 Rogers 5870	0.30×0.30×0.017	41	84	Introducing an antipodal Y-strip with a square slot antenna
[24] 2018	6.03,6.1 FR4	0.32×0.23×0.015	55	42	Vertically extending one side of the ground plane, while a cross-shaped monopole structure and the presence of a slot in the ground plane
Proposed 2018	**3.48,3.12**	**0.33×0.33×0.012**	**56**	**63.61**	**Inverted L strip and hook-shaped rectangular ground plane**

TABLE 3. Performance of the proposed antenna by scaling the dimensions.

Target Frequency (GHz)	Patch dimension (Theoretical) in mm	Overall Designed Dimension (mm)	Impedance Bandwidth	AR Bandwidth	Applications
2.25	40.17×31.07×1.6	44×44×1.6	2.25-4.0 (56%)	2.38-4.6 (63.61%)	ISM, WiMAX, WLAN, satellite communications, cordless telephones, weather radar systems and lower frequency bands CP type applications
1.50	60.66×47.17×1.6	66×66 ×1.6	1.49-2.63 (55.33%)	1.57-3.10(65.52%)	GPS, WLAN, ISM Applications
1.10	81.43×63.46×1.6	88×88 ×1.6	1.11-1.95 (54.90%)	1.14-2.47(73.68%)	GPS, GNS, ISM, WLAN
3.60	24.88×18.98×1.6	22×22 ×1.6	3.6-6.65(59.91%)	4.17-6.25(39.92%)	C band Applications

AR bandwidth is approximately 2.19 GHz (2.38-4.58 GHz), which is approximately 63.23% at 3.48 GHz. The computer-generated (using HFSS) and measured radiation pattern are demonstrated in Figure 13 at 2.4 and 3.5 GHz, respectively. With opposite sense (RHCP and LHCP) polarization, the antenna radiates a bidirectional wave. The antenna is radiated towards the LHCP for Z > 0 and the RHCP for Z < 0. It is perceived that at both frequencies, the main beam direction hardly shifts away from the peak. The antenna's measured and simulated (HFSS) gains are depicted in Figure 14. The average measured gain is more than 2.98 dBic in the achieved operating band, and the measured peak gain is approximately 3.54 dBic at 3.70 GHz. Simulated and measured radiation efficiency of the realized antenna is demonstrated in Fig. 15. The radiation efficiency in the measured and simulation for the desired band is higher than 85%.

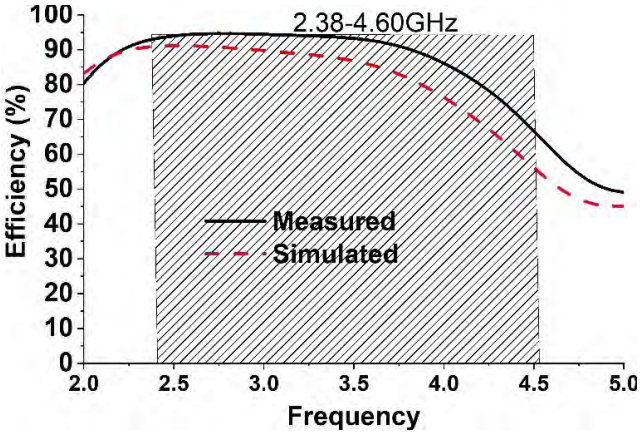

FIGURE 15. Simulated and measured radiation efficiency against frequency.

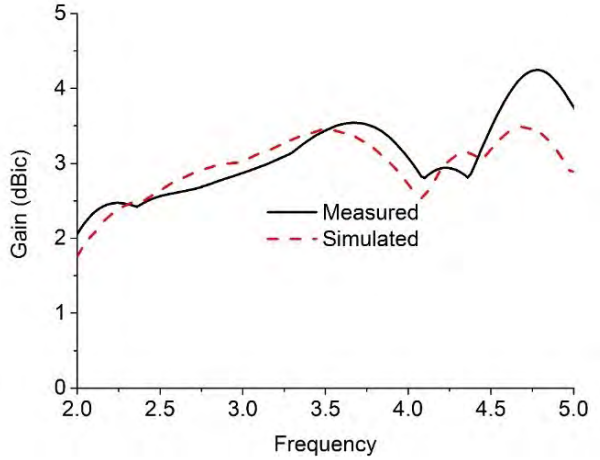

FIGURE 14. Simulated and measured gain against frequency.

For the comparison of the performance of the optimized antenna, the −10dB impedance bandwidth (BW), the axial ratio bandwidth (ARBW), antenna dimension and the state of the art of the reported antennas to achieve a wide AR and impedance bandwidth in the literature review are summarized in Table 2. The force and fear are the center frequency of the impedance bandwidth and 3 dB axial ratio bandwidth, and λ_o is the corresponding free space wavelength. It can be observed from the table that the proposed antenna occupies a smaller area and possess a wider CP bandwidth than existing reported antennas. Table 3 presents the impedance and axial ratio performance of the proposed design (Antenna 3) for the different scaling dimension (L) only. From this table, it can be perceived that the wide impedance (approximately 56) and AR bandwidth (approximately 63%) have been achieved for the scaling dimension (L) without changing the other antenna parameters. If the designed parameters, such as g_1, g_2, W_1, W_2, d_1, g_x, and g_y, can be tuned, the impedance and AR bandwidth can also be increased. Thus, any researcher can be easily redesigned for any desired wide CP operating

band application through the scaling dimension (L) without changing the shape, which is the novelty of the presented antenna.

V. CONCLUSION

In this article, a novel hook-shaped printed patch antenna with a wideband CP radiation pattern property has been presented. The antenna is comprised of the reversed asymmetric arm L-shaped microstrip feed with the hook-shaped branch ground plane. The surface current movements are swapped by interleaving a hook-shaped branch in the ground plane to stimulate the CP. By tuning the length and width of the ground plane and the gap between the inverted L-shaped feed and the hook-shaped branch, the impedance and AR bandwidth is widely achieved. The measured impedance and AR bandwidths are given as 56% and 63.61%, respectively. The proposed antenna exhibits a good symmetry with an opposite sense bi-directional radiation with LHCP (left-hand circular polarization) in the +Z direction and RHCP (right-hand circular polarization) in the −Z direction with an average peak gain of 2.98 dBic. Because of its compact size, structural simplicity and bidirectional broadband CP characteristics, the proposed antenna can have real-world applications for numerous multiband circular polarization systems. Thus, any researcher can redesign the required CP operating band application antenna with only scaling the dimension (L) of the proposed antenna without changing the other parameters. Since, the designed antenna is also highly compact and low-profile with broad CP characters and is an auspicious candidate for a wide selection of wireless applications.

REFERENCES

[1] S. Gao, Q. Luo, and F. Zhu, *Circularly Polarized Antennas*. Hoboken, NJ, USA: Wiley, 2014.
[2] A. K. Bhattacharyya and L. Shafai, "A wider band microstrip antenna for circular polarization," *IEEE Trans. Antennas Propag.*, vol. AP-36, no. 2, pp. 157–163, Feb. 1988.
[3] X. L. Bao and M. J. Ammann, "Comparison of several novel annular-ring microstrip patch antennas for circular polarization," *J. Electromagn. Waves Appl.*, vol. 20, no. 11, pp. 1427–1438, 2006.
[4] Y. M. Pan, S. Y. Zheng, and B. J. Hu, "Wideband and low-profile omnidirectional circularly polarized patch antenna," *IEEE Trans. Antennas Propag.*, vol. 62, no. 8, pp. 4347–4351, Aug. 2014.
[5] X. L. Bao, M. J. Ammann, and P. McEvoy, "Microstrip-fed wideband circularly polarized printed antenna," *IEEE Trans. Antennas Propag.*, vol. 58, no. 10, pp. 3150–3156, Oct. 2010.
[6] T.-N. Chang, "Wideband circularly polarised antenna using two linked annular slots," *Electron. Lett.*, vol. 47, no. 13, pp. 737–739, 2011.
[7] T. N. Chang and J. M. Lin, "Wideband circularly polarised antenna on slot-loaded ground plane," *Electron. Lett.*, vol. 48, no. 14, pp. 818–819, Jul. 2012.
[8] K. G. Thomas and G. Praveen, "A novel wideband circularly polarized printed antenna," *IEEE Trans. Antennas Propag.*, vol. 60, no. 12, pp. 5564–5570, Dec. 2012.
[9] L. Zhang, Y.-C. Jiao, Y. Ding, B. Chen, and Z.-B. Weng, "CPW-fed broadband circularly polarized planar monopole antenna with improved ground-plane structure," *IEEE Trans. Antennas Propag.*, vol. 61, no. 9, pp. 4824–4828, Sep. 2013.
[10] Y.-M. Cai, K. Li, Y.-Z. Yin, and W. Hu, "Broadband circularly polarized printed antenna with branched microstrip feed," *IEEE Antennas Wireless Propag. Lett.*, vol. 13, pp. 674–677, 2014.
[11] T. Fujimoto and K. Jono, "Wideband rectangular printed monopole antenna for circular polarisation," *IET Microw. Antennas Propag.*, vol. 8, no. 9, pp. 649–656, 2014.
[12] M. Samsuzzaman and M. T. Islam, "Wideband hook-shaped circularly polarised antenna," *Electron. Lett.*, vol. 50, no. 15, pp. 1043–1045, 2014.
[13] Q. W. Lin, H. Wong, X. Y. Zhang, and H. W. Lai, "Printed meandering probe-fed circularly polarized patch antenna with wide bandwidth," *IEEE Antennas Wireless Propag. Lett.*, vol. 13, pp. 654–657, 2014.
[14] S. Fu, Q. Kong, S. Fang, and Z. Wang, "Broadband circularly polarized microstrip antenna with coplanar parasitic ring slot patch for L-band satellite system application," *IEEE Antennas Wireless Propag. Lett.*, vol. 13, pp. 943–946, 2014.
[15] G. Li, H. Zhai, L. Li, and C. Liang, "A nesting-L slot antenna with enhanced circularly polarized bandwidth and radiation," *IEEE Antennas Wireless Propag. Lett.*, vol. 13, pp. 225–228, 2014.
[16] J. Shen, C. Lu, W. Cao, J. Yang, and M. Li, "A novel bidirectional antenna with broadband circularly polarized radiation in X-band," *IEEE Antennas Wireless Propag. Lett.*, vol. 13, pp. 7–10, 2014.
[17] A. Panahi, X. L. Bao, G. Ruvio, and M. J. Ammann, "A printed triangular monopole with wideband circular polarization," *IEEE Trans. Antennas Propag.*, vol. 63, no. 1, pp. 415–418, Jan. 2015.
[18] B. Hu and Z. Shen, "Broadband circularly polarized moon-shaped monopole antenna," *Microw. Opt. Technol. Lett.*, vol. 57, no. 5, pp. 1135–1139, 2015.
[19] M. S. Ellis, Z. Zhao, J. Wu, X. Ding, Z. Nie, and Q.-H. Liu, "A novel simple and compact microstrip-fed circularly polarized wide slot antenna with wide axial ratio bandwidth for C-band applications," *IEEE Trans. Antennas Propag.*, vol. 64, no. 4, pp. 1552–1555, Apr. 2016.
[20] R. C. Han, and S.-S. Zhong, "Broadband circularly-polarised chifre-shaped monopole antenna with asymmetric feed," *Electron. Lett.*, vol. 52, no. 4, pp. 256–258, Feb. 2016.
[21] R. K. Saini and S. Dwari, "A broadband dual circularly polarized square slot antenna," *IEEE Trans. Antennas Propag.*, vol. 64, no. 1, pp. 290–294, Jan. 2016.
[22] X. Ren, S. Liao, and Q. Xue, "Design of wideband circularly polarized Vivaldi antenna with stable radiation pattern," *IEEE Access*, vol. 6, pp. 637–644, 2018.
[23] M. Nosrati and N. Tavassolian, "Miniaturized circularly polarized square slot antenna with enhanced axial-ratio bandwidth using an antipodal Y-strip," *IEEE Antennas Wireless Propag. Lett.*, vol. 16, pp. 817–820, 2017.
[24] K. O. Gyasi *et al.*, "A compact broadband cross-shaped circularly polarized planar monopole antenna with a ground plane extension," *IEEE Antennas Wireless Propag. Lett.*, vol. 17, no. 2, pp. 335–338, Feb. 2018.
[25] X. Chen, L. Wang, D. Wu, J. Lei, and G. Fu, "Compact and wideband directional circularly polarized distributed patch antenna with high efficiency," *IEEE Access*, vol. 5, pp. 15942–15947, 2017.

MD. SAMSUZZAMAN was born in Jhenaidah, Bangladesh, in 1982. He received the B.Sc. and M.Sc. degrees in computer science and engineering from Islamic University Kushtia, Bangladesh, in 2005 and 2007, respectively, and the Ph.D. degree from Universiti Kebangsaan Malaysia, Malaysia, in 2015. From 2008 to 2011, he was a Lecturer at Patuakhali Science and Technology University, Bangladesh. From 2011 to 2015, he was an Assistant Professor at Patuakhali Science and Technology University, where he is currently an Associate Professor. He is currently a Post-Doctoral Fellow at Universiti Kebangsaan Malaysia. He has authored and co-authored about 80 research journal articles, nearly 20 conference articles, and a few book chapters on various topics related to antennas, microwaves and electromagnetic radiation analysis with one inventory patents filed. His Google scholar citation is 546 and H-index is 13. His research interests include the communication antenna design, satellite antennas, and microwave imaging.

MOHAMMAD TARIQUL ISLAM (SM'08) is currently a Professor at the Department of Electrical, Electronic and Systems Engineering, Universiti Kebangsaan Malaysia (UKM), and a Visiting Professor at the Kyushu Institute of Technology, Japan. He has authored and co-authored about 350 research journal articles, nearly 165 conference articles, and a few book chapters on various topics related to antennas, microwaves and electromagnetic radiation analysis with 16 inventory patents filed. Thus far, his publications have been cited 4210 times and his H-index is 33 (Source: Scopus). His Google scholar citation is 5545 and H-index is 36. His research interests include communication antenna design, radio astronomy antennas, satellite antennas, and electromagnetic radiation analysis. He is a member of IET, U.K., and IEICE, Japan. He is a Chartered Professional Engineer-CEng. He was a recipient of over 40 research grants from the Malaysian Ministry of Science, Technology and Innovation, Ministry of Education, UKM Research Grant, and international research grants from Japan and Saudi Arabia. He was also a recipient of the Publication Award from the Malaysian Space Agency in 2009, 2010, 2013, and 2014, respectively, and the Best Paper Presentation Award in 2012 International Symposium on Antennas and Propagation, (ISAP 2012) at Nagoya, Japan, and at IconSpace in 2015. He received several international gold medal awards, a Best Invention in Telecommunication Award, a Special Award from Vietnam for his research and innovation, and Best Researcher Awards in 2010 and 2011 at UKM. He also received the Best Innovation Award in 2011 and the Best Research Group in ICT niche by UKM in 2014. He currently serves as the Editor-in-Chief for the *International Journal of Electronics, Informatics* and an Associate Editor for *Electronics Letter*.

MANDEEP JIT SINGH received the B.Eng. (Hons.) and Ph.D. degrees in electrical and electronic engineering from the University of Notrhumbria, U.K., and Universiti Sains Malaysia, in 1998 and 2006, respectively. From 2006 to 2009, he was at Universiti Sains Malaysia as a Lecturer. He is currently at Universiti Kebangsaan Malaysia as an Associate Professor. He has published 190 papers in ISI journals. He has reviewed over 200 articles in impact factors journal. His areas of specialization are radiowave propagation in satellite communication system and RFID antenna design. His collaborated with the Association of Radio Industries and Business, Japan, to analyze the rain fade at Ku-band in tropical climate using satellite involving countries, such as Thailand, Philippines, Indonesia, and Fiji. Current collaboration is with the National Defense Agency, Japan, Microwave Anechoic Lab Chamber, and Kyutech University on antenna development.